

Noise Analysis of a Multispectral Image Acquisition System

Noriyuki Shimano, Department of Informatics, School of Science and Engineering, Kinki University, 3-4-1, Kowakae, Higashi-Osaka, Osaka 577-8502, Japan, e-mail: shimano@info.kindai.ac.jp

Abstract

Prior knowledge of the noise present in a color image acquisition device is very important for the recovery of a spectral reflectance of an object being imaged, since the recovery performance is greatly influenced by the noise.

In the previous paper (IEEE Trans. Image Process. 15, 1848 (2006)), the author proposed a new model to estimate the noise variance of an image acquisition system by assuming that the noise variance in each channel is equal and showed that this model is very useful to accurately recover a spectral reflectance of an imaged object. This paper describes an extended model for the estimation of the covariance matrix of the noise present in an image acquisition system without the assumption. It is demonstrated that the proposal overfits the noise covariance matrix to learning samples and that the recovery performance for the test samples is poor compared with the previous model. However this overfitting means that the estimates are correctly performed using the proposed model. The new model is effective in analyzing the noise present in an image acquisition system.

Introduction

The noise plays important roles in an image acquisition such as the solutions to the inverse problems [1]-[4], the optimization of a set of sensors [5] and the evaluation of a set of sensors aimed at acquisition of spectral information [6] and colorimetric information [7]. The noise in solving inverse problems must be defined to include all sensor response errors resulting not only from the CCD itself but also from the inaccuracies in the sampled spectral characteristics of sensors, reflectances of objects and illuminations and from the quantization of sensor responses, etc. The noise defined above was termed as the system noise [8].

As the least square error estimation, the Wiener estimation is usually used in solving the inverse problems. Prior knowledge of the spectral reflectances of the imaged objects and the noise present in the image acquisition system, i.e., the system noise, is required for the estimation. However the knowledge is usually unknown and it is impossible to use the Wiener estimation in solving inverse problems in the actual cases. The author already proposed a new model for the estimation of the system noise variance using measured spectral reflectances of the learning samples and their corresponding image data [8]. The estimated noise variance agrees fairly well with the noise variance that minimizes the value of the mean square error (MSE) between the measured and the recovered spectral reflectances of the learning samples.

The estimated system noise variance and the autocorrelation matrix of the spectral reflectances of the learning samples can be used to recover the spectral reflectances of the test samples without prior knowledge of them. The accuracies of the recovered spectral reflectances were compared with other recovery models, and it is found that the recovered spectral reflectances by the Wiener estimation

with the proposed model [8] are more accurate than the others when the test samples are different from learning samples [9]. In the learning model, the evaluation of the computational efficiency, robustness and statistical stability are very important [10]. The robustness means that the learning algorithms must handle noisy data for real applications and the statistical stability means that the performance of the algorithms should not be sensitive to the particular training data set. The performance of the regression model [11],[12] is not enough for test samples, since the model overfits the system noise to learning samples [9]. On the other hand the previously proposed model gives the robustness to the noise and statistical stability [8],[9].

In the previous model, the system noise was assumed independent, identically distributed (i.i.d) random variables over each channel. However the noise variance of each channel is not always equal. Recovery performances of the previous and new models were compared. It was found that the recovery performance of the new model is superior to that of previous model when the same samples were used for training and test samples and that the recovery performance of the new model is poor compared with previous model when test samples are different from training samples, since the new model overfits the covariance matrix to training samples. However this overfitting means that the estimates of the covariance matrix are performed correctly. In this paper the noise present in a multispectral camera was analyzed using the new proposal and shows that the proposal is very important for the analysis of the influence of the signal power, quantization and sampling intervals (over the visible wavelengths) on the noise variance.

Model

In this section, a model estimating an covariance matrix of the system noise is discussed based on the Wiener estimation, since it provides us with a method for the confirmation of the accuracy of the estimates by comparing the recovered spectral reflectances [8].

A vector space notation is usually used for the formulation of the problems and the visible wavelengths are sampled at constant intervals and the sampling number is denoted N . A sensor response vector from a set of color sensors for an object with an $N \times 1$ spectral reflectance vector \mathbf{r} can be expressed by

$$\mathbf{p} = \mathbf{S}\mathbf{L}\mathbf{r} + \mathbf{e} \quad (1)$$

where \mathbf{p} is an $M \times 1$ sensor response vector from the M channel sensors, \mathbf{S} is an $M \times N$ matrix of the spectral sensitivities of sensors in which a row vector represents a spectral sensitivity of a sensor, \mathbf{L} is an $N \times N$ diagonal matrix with samples of the spectral power distribution of an illuminant along the diagonal, \mathbf{e} is an $M \times 1$ additive system noise vector as stated above. Object-dependent noise and object-independent noise have been considered in an image acquisition device [13]. The former noise results from the shot

noise accompanied with the incidence of intense light into a CCD and was observed from the CCD signals [14],[15]. The latter noise is usually used for the analysis of color image acquisition [16] and was used to solve inverse problems[17],[18]. However, from the previous work on the system noise, the system noise can be considered as the object independent, since the experimental results agree quite well with the model based on the assumption of the object independence [8]. In this context, the assumptions that \mathbf{r} and \mathbf{e} are uncorrelated and the noise-mean is zero are reasonable. For abbreviation, let $S_L = SL$ below. The recovered spectral reflectance vector $\hat{\mathbf{r}}$ can be given by the Wiener estimation.

$$\hat{\mathbf{r}} = R_{SS} S_L^T (S_L R_{SS} S_L^T + R_{ges})^{-1} \mathbf{p}, \quad (2)$$

where T represents the transpose of a matrix, R_{SS} is an autocorrelation matrix of the spectral reflectances of samples which will be captured by a device and the R_{SS} is expressed by $R_{SS} = E\{\mathbf{r}\mathbf{r}^T\}$, where $E\{\bullet\}$ represents an expectation value. R_{ges} in Eq.(2) represents a covariance matrix of the noise used for the Wiener estimation. If R_{ges} is equal to the covariance matrix of the system noise, i.e., $R_{ges} = R_{ee} = E\{\mathbf{e}\mathbf{e}^T\}$, then the Wiener estimation gives the most accurate recovery. However, since prior knowledge of the noise is not usually available, usually R_{ges} is simply a guess. The estimation error vector $\Delta\mathbf{r}$ between an actual \mathbf{r} and a recovered vector $\hat{\mathbf{r}}$ for a surface reflectance is given by

$$\Delta\mathbf{r} = \mathbf{r} - \hat{\mathbf{r}}. \quad (3)$$

Since the autocorrelation matrix R_{SS} of surface reflectance spectra is symmetrical, it is represented by a set of eigenvectors and eigenvalues of the matrix as $R_{SS} = V\Lambda V^T$, where V represents the basis matrix, i.e., it is expressed by $V = (\mathbf{v}_1 \ \mathbf{v}_2 \ \dots \ \mathbf{v}_N)$, where $\{\mathbf{v}_i\}_{i=1, \dots, N}$ represent a set of eigenvectors of an autocorrelation matrix. Λ is an $N \times N$ diagonal matrix with positive eigenvalues of the matrix along the diagonal in decreasing order. Let $S_L^V = S_L V \Lambda^{1/2}$. The recovered spectral reflectance $\hat{\mathbf{r}}$ when $R_{ges} = 0$, i.e., all elements of the matrix R_{ges} are zero, is expressed by the substitution of the relations of $R_{SS} = V\Lambda V^T$ and $S_L^V = S_L V \Lambda^{1/2}$ into Eq. (2) as

$$\hat{\mathbf{r}} = V \Lambda^{1/2} S_L^V T (S_L^V S_L^V T)^{-1} \mathbf{p}. \quad (4)$$

The singular value decomposition (SVD) of the matrix of S_L^V can be written by $S_L^V = \sum_{i=1}^{\beta} \kappa_i^y \mathbf{d}_i^y \mathbf{b}_i^y T$, where $\beta = \text{Rank}(S_L^V)$, and κ_i^y , \mathbf{d}_i^y and \mathbf{b}_i^y represent the i -th singular value, the i -th left and right singular vector, respectively. Then, the term $S_L^V T (S_L^V S_L^V T)^{-1}$ in Eq. (4) can be expressed by $S_L^V T (S_L^V S_L^V T)^{-1} = \sum_{i=1}^{\beta} \kappa_i^{y-1} \mathbf{b}_i^y \mathbf{d}_i^y T$. Substitution of the expression into Eq. (4) and combining Eqs.(1) and (3) leads to

$$\Delta\mathbf{r} = \mathbf{r} - V \Lambda^{1/2} \sum_{i=1}^{\beta} \kappa_i^{y-1} \mathbf{b}_i^y \mathbf{d}_i^y T (S_L \mathbf{r} + \mathbf{e}). \quad (5)$$

The mean of the autocorrelation matrix of $\Delta\mathbf{r}$ for many spectral reflectances is given by

$$E\{\Delta\mathbf{r}\Delta\mathbf{r}^T\} = E\left\{\left(\mathbf{r} - V \Lambda^{1/2} \sum_{i=1}^{\beta} \kappa_i^{y-1} \mathbf{b}_i^y \mathbf{d}_i^y T (S_L \mathbf{r} + \mathbf{e})\right) \times \left(\mathbf{r} - V \Lambda^{1/2} \sum_{i=1}^{\beta} \kappa_i^{y-1} \mathbf{b}_i^y \mathbf{d}_i^y T (S_L \mathbf{r} + \mathbf{e})\right)^T\right\}. \quad (6)$$

Let denote the autocorrelation matrix of $E\{\Delta\mathbf{r}\Delta\mathbf{r}^T\}$ as $A(R_{ges}, R_{ee})$, then $A(0, R_{ee})$, i.e., the autocorrelation matrix when $R_{ges} = 0$, is given by (for more detail see APPENDIX A)

$$A(0, R_{ee}) = V \Lambda V^T - \sum_{i=1}^{\beta} V \Lambda^{1/2} \mathbf{b}_i^y \mathbf{b}_i^y T \Lambda^{1/2} V^T + \sum_{i=1}^{\beta} \sum_{j=1}^{\beta} \kappa_i^{y-1} \kappa_j^{y-1} V \Lambda^{1/2} \mathbf{b}_i^y \mathbf{d}_i^y T R_{ee} \mathbf{d}_j^y \mathbf{b}_j^y T \Lambda^{1/2} V^T \quad (7)$$

The first and second term on the right hand side of Eq.(7) represent the noise independent terms and the third term represents the noise dependent term. Eq. (7) can be rewritten as

$$\sum_{i=1}^{\beta} \sum_{j=1}^{\beta} \kappa_i^{y-1} \kappa_j^{y-1} \mathbf{b}_i^y \mathbf{d}_i^y T R_{ee} \mathbf{d}_j^y \mathbf{b}_j^y T = \Lambda^{-1/2} V^T \left(A(0, R_{ee}) - V \Lambda V^T + \sum_{i=1}^{\beta} V \Lambda^{1/2} \mathbf{b}_i^y \mathbf{b}_i^y T \Lambda^{1/2} V^T \right) V \Lambda^{-1/2}. \quad (8)$$

By multiplying both sides of (8) by vectors $\mathbf{b}_m^y T$ and \mathbf{b}_n^y from left and right sides, respectively, then the use of the orthogonal normality of singular vectors leads next equation

$$\mathbf{d}_m^y T R_{ee} \mathbf{d}_n^y = \kappa_m^y \kappa_n^y \mathbf{b}_m^y T \Lambda^{-1/2} V^T \times \left(A(0, R_{ee}) - V \Lambda V^T + \sum_{i=1}^{\beta} V \Lambda^{1/2} \mathbf{b}_i^y \mathbf{b}_i^y T \Lambda^{1/2} V^T \right) V \Lambda^{-1/2} \mathbf{b}_n^y. \quad (9)$$

Note both sides of (9) represent the scalar. By multiplying both sides of (9) by vectors \mathbf{d}_m^y and $\mathbf{d}_n^y T$ from left and right hand sides, respectively, and summing both sides over m and n , by using the relation of $\sum_{i=1}^{\beta} \mathbf{d}_i^y \mathbf{d}_i^y T = I_{\beta}$, where I_{β} represents the $\beta \times \beta$ identity matrix, then the autocorrelation of the system noise R_{ee} can be expressed as,

$$\hat{R}_{ee} = \sum_{m=1}^{\beta} \sum_{n=1}^{\beta} \kappa_m^y \kappa_n^y \mathbf{b}_m^y T \Lambda^{-1/2} V^T \times \left(A(0, R_{ee}) - V \Lambda V^T + \sum_{i=1}^{\beta} V \Lambda^{1/2} \mathbf{b}_i^y \mathbf{b}_i^y T \Lambda^{1/2} V^T \right) V \Lambda^{-1/2} \mathbf{b}_n^y \mathbf{d}_n^y T \quad (10)$$

The above equation can be simplified using the orthogonal normality of singular vectors as,

$$\hat{R}_{ee} = \sum_{m=1}^{\beta} \sum_{n=1}^{\beta} \kappa_m^y \kappa_n^y \mathbf{b}_m^y T \Lambda^{-1/2} V^T A(0, R_{ee}) V \Lambda^{-1/2} \mathbf{b}_n^y \mathbf{d}_n^y T. \quad (11)$$

The factor $A(0, R_{ee})$ on the right hand side of Eq.(11) can be obtained by recovering spectral reflectances $\hat{\mathbf{r}}$ by the Wiener filter with $R_{ges} = 0$ and averaging the autocorrelation of the error $(\mathbf{r} - \hat{\mathbf{r}})(\mathbf{r} - \hat{\mathbf{r}})^T$ over all learning samples, where \mathbf{r} represents a measured spectral reflectance. Other factors on the right hand side can be computed by the spectral characteristics of sensors, illumination and reflectances of the learning samples. Therefore, Eq.(11) gives a formula to estimate the covariance matrix of the system noise. It is very important to note that the spectral reflectances recovered by the Wiener estimation with \hat{R}_{ee} is designed to minimize the MSE, since the MSE of the spectral reflectances recovered by the Wiener estimation is minimized when $R_{ges} = R_{ee} = E\{\mathbf{e}\mathbf{e}^T\}$ and the \hat{R}_{ee} (in Eq.(11)) is the formulation of $R_{ee} = E\{\mathbf{e}\mathbf{e}^T\}$ including $A(0, R_{ee})$.

Experimental Procedures and Results

Experimental Procedures

The same experimental data applied in the previous paper [8] were used for the comparison of the recovery performances. More detailed experimental conditions and procedures are described in the previous paper. In short, experimental conditions and procedures are summarized below. A multispectral image acquisition system was assembled using eight interference filters (Asahi Spectral Corporation) in conjunction with a monochrome video camera (SONY XC-75) with an optical lens (CANON zoom lens V6×16). The Kodak Q60R1 and the GretagMacbeth ColorChecker were illuminated by halogen lamp, and their image data were captured by the multispectral camera. The image data from the video camera were converted to 8bit-depth digital data by an AD converter. The sampling intervals of 10nm were used over the wavelengths from 400 to 700nm (N=31) in this paper for the spectral characteristics of sensors, illumination and reflectances. Fig.1 shows the spectral sensitivities of sensors used for image capture. Fig.1(a) and (b) show the spectral sensitivities of a set of sensors used for Kodak Q60R1 and GretagMacbeth ColorChecker, respectively. A halogen lamp was used for image acquisition and its spectral power distribution is shown in Fig.2.

Experimental Results of the Estimates of the Covariance Matrix

Before showing the experimental results, it is better to explain the previous model [8]. In the previous model, the noise covariance matrix R_{ges} in Eq.(2) was assumed as the product of the noise variance σ_e^2 and the identity matrix I , i.e., the assumption of $R_{ges} = \sigma_e^2 I$ was used. By changing the noise variance σ_e^2 for the Wiener estimation to recover the spectral reflectance \hat{r} , the MSE between the measured spectral reflectance and the recovered reflectance is calculated by $E\{\|r - \hat{r}\|^2\}$ for all reflectance r . The variance σ_e^2 that minimizes the MSE is called as the optimum noise variance σ_{opt}^2 . The optimum noise variance is considered as the actual system noise variance, since the values of the MSE is minimized when $\sigma_e^2 = \sigma^2$, where σ^2 represents the actual system noise variance (for more detail, see Eqs.(8) and (9) in ref.8).

Table I shows the estimated results for the Kodak Q60R1 and the GretagMacbeth ColorChecker. In the table, $MSE(\sigma_{opt}^2 I, R_{ee})$ is the MSE at $R_{ges} = \sigma_{opt}^2 I$ that minimizes the MSE, $MSE(\hat{\sigma}^2 I, R_{ee})$ is the MSE at $R_{ges} = \hat{\sigma}^2 I$ estimated by the previous model [8], $MSE(\hat{R}_{ee}, R_{ee})$ is the MSE at $R_{ges} = \hat{R}_{ee}$ estimated by Eq.(11) and the value of the $Tr(R_{ee})/M$ represents the trace of the \hat{R}_{ee} divided by the M . A bold-faced letter in each row of the table shows the minimum value of the MSE. The results show that the values of the $MSE(\hat{R}_{ee}, R_{ee})$ are smaller than that of the $MSE(\sigma_{opt}^2 I, R_{ee})$ and $MSE(\hat{\sigma}^2 I, R_{ee})$ when the same samples are used for the training and test samples and that the \hat{R}_{ee} is correctly formulated. However, when different samples are used for training and test samples, the previous model outperforms the new proposal. The results show that the new proposal overfits the noise covariance matrix to learning samples and that this overfitting means that the estimates are correctly performed using proposed model. Fig.3 shows typical experimental results of the spectral reflectance recovered by the previous and new models. From the experimental results the spectral reflectance recovered by the new proposal is more accurate than that by the previous model when the same samples are used for learning and test samples.

Since the new proposal gives the noise variance for each channel, signal power dependence of the noise variance can

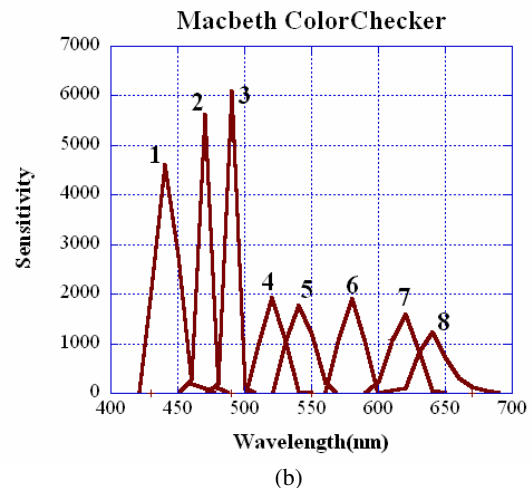
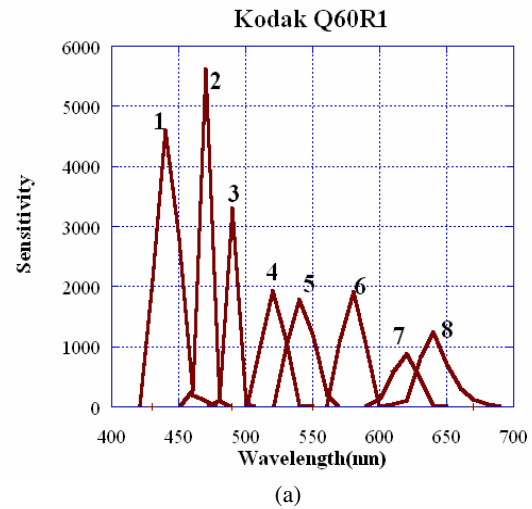


Figure 1. Spectral sensitivities of a set of sensors used for image capture. Figure (a) and (b) represent the spectral sensitivities used for Kodak Q60R1 and Macbeth ColorChecker, respectively

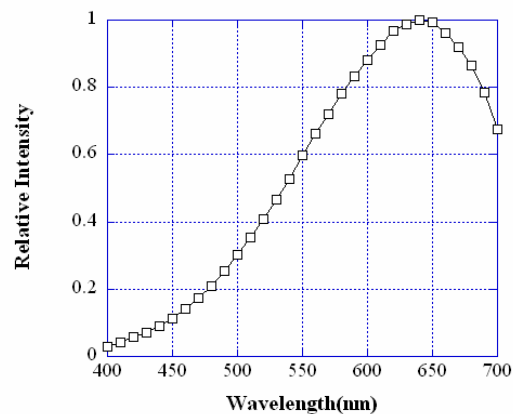


Figure 2. Spectral power distribution of a halogen lamp used for image acquisition

Table 1 Estimated parameters

Training	Test	$MSE(\hat{\sigma}_{opt}^2 I, R_{ee})$	$MSE(\hat{\sigma}^2 I, R_{ee})$	$MSE(\hat{R}_{ee}, R_{ee})$	σ_{opt}^2	$\hat{\sigma}^2$	$Tr(\hat{R}_{ee})/M$
KodakQ60	KodakQ60	0.014799	0.014974	0.011739	5.26e-004	2.91e-004	6.72e-004
Macbeth	Macbeth	0.038457	0.038568	0.033286	4.79e-004	3.90e-004	6.31e-004
KodakQ60	Macbeth	-	0.074551	0.098864	-	2.91e-004	6.72e-004
Macbeth	Kodak Q60	-	0.049293	0.057238	-	3.90e-004	6.31e-004

be studied by averaging signal power for each channel. Fig.4 shows the noise variance as a function of the averaged signal power. From the results, it is concludes that the noise variance has no correlation with the signal power.

To study the influence of the quantization and sampling intervals on the noise variance, image data from CCD camera (Kodak KAI-4021M) were converted to 16-bit-depth digital data by an AD converter. The spectral characteristics of the sensitivities, illuminations (Seric Solax XC-100AF) and reflectances (Macbeth) were measured over wavelengths from 400 to 700 nm at 1-nm intervals. Fig.5 shows the noise variance as a function of the sampling intervals (over the visible wavelengths) and quantization bit-depth (converting sensor responses from analog signals to digital), where trace of

the estimated correlation matrix R_{ee} divided by the channel number M , i.e. $Tr(\hat{R}_{ee})/M$, is used for the noise variance. The experimental results show that the system noise variance increases with a decrease in the quantization bit-depth below 8 bit and increases with an increase in the sampling interval longer than 20nm.

A more direct and simple estimation of the system noise variance has been performed by using Eq.(1) in the previous paper [8]. The noise variance estimated by $\hat{\sigma}^2 = M^{-1}E\{\|p - S_{tr}\|^2\}$ is not enough to accurately recover the spectral reflectances, since the estimates by this method directly reflect the errors in computing a sensor response $p = S_{tr}r$ using the measured spectral characteristics of the sensors, illumination and

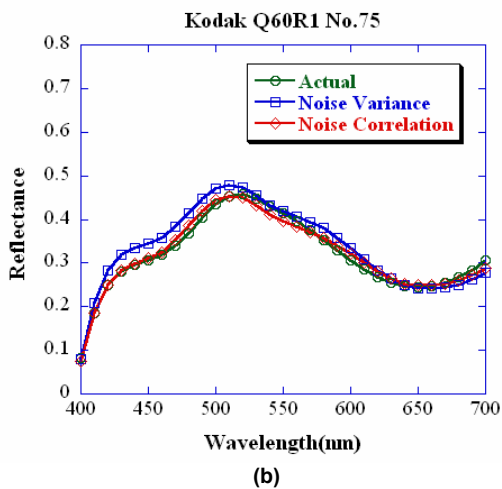
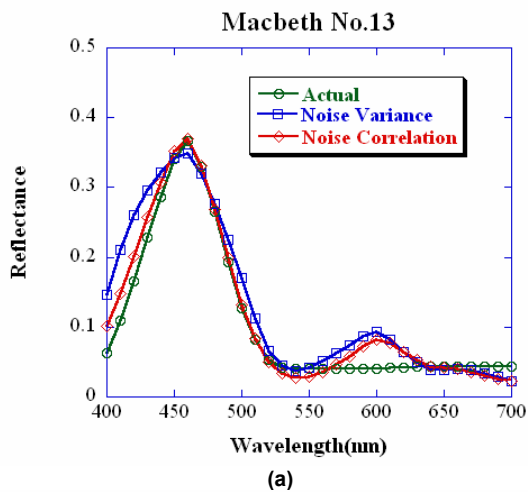


Figure 3. Spectral reflectances recovered by the new and previous model. Figs(a) and (b) show results for Macbeth ColorChecker No. 13 and Kodak Q60R1No.75, respectively

Eight Channels Camera for Kodak Q60R1

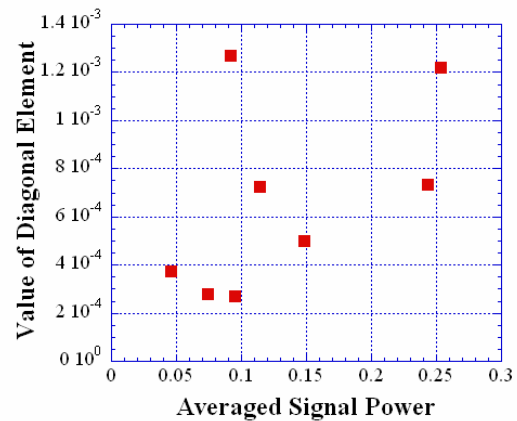


Figure 4. Noise variance as a function of averaged signal power in each channel

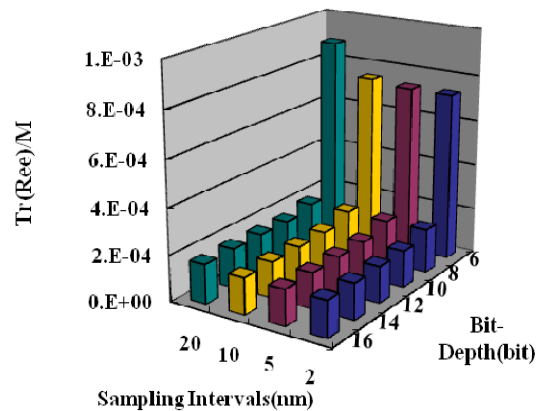


Figure 5. The influence of sampling intervals and the quantization bit depth of the sensor responses on the Trace of R_{ee} divided with channel number

reflectance of a color (for more detail see ref.8). The same thing is true for the estimates by $\hat{R}_{cc} = E\left\{(\mathbf{p} - S_L \mathbf{r})(\mathbf{p} - S_L \mathbf{r})^T\right\}$.

Conclusion

A new model is proposed for the estimation of the covariance matrix of the system noise of a color image acquisition system and it was applied to a multispectral image acquisition system to show the trustworthiness of the proposal. From the experimental results on the proposed model show that the system noise is largely uncorrelated and is not identically distributed in each channel. Since the covariance matrix estimated by the proposal overfits the matrix to learning samples, the recovery performance for test samples is poor compared with the previous model. However this over fitting means that the estimates of the covariance matrix are correctly performed using the proposed model. The proposal is very important for the noise analysis of an image acquisition system.

Acknowledgements

This research was partially supported by the Japan Society for the Promotion of Science, Grant-in-Aid for Scientific Research (C) 20500173, 2009.

APPENDIX A: DERIVATION OF Eq. (7)

For many surface reflectances, the autocorrelation matrix of the error vector $\Delta \mathbf{r}$ is averaged over the surface reflectance spectra and it is given by

$$E\{\Delta \mathbf{r} \Delta \mathbf{r}^T\} = E\left\{\left(\mathbf{r} - V\Lambda^{1/2} \sum_{i=1}^{\beta} \kappa_i^{-1} \mathbf{b}_i^y \mathbf{d}_i^y{}^T (S_L \mathbf{r} + \mathbf{e})\right) \bullet \left(\mathbf{r} - V\Lambda^{1/2} \sum_{i=1}^{\beta} \kappa_i^{-1} \mathbf{b}_i^y \mathbf{d}_i^y{}^T (S_L \mathbf{r} + \mathbf{e})\right)^T\right\}. \quad (A1)$$

The above equation can be rewritten as

$$\begin{aligned} E\{\Delta \mathbf{r} \Delta \mathbf{r}^T\} &= E\left\{\left(\left(\mathbf{I} - V\Lambda^{1/2} \sum_{i=1}^{\beta} \kappa_i^{-1} \mathbf{b}_i^y \mathbf{d}_i^y{}^T S_L\right) \mathbf{r} - \left(V\Lambda^{1/2} \sum_{i=1}^{\beta} \kappa_i^{-1} \mathbf{b}_i^y \mathbf{d}_i^y{}^T\right) \mathbf{e}\right) \right. \\ &\quad \times \left. \left(\mathbf{r}^T \left(\mathbf{I} - V\Lambda^{1/2} \sum_{i=1}^{\beta} \kappa_i^{-1} \mathbf{b}_i^y \mathbf{d}_i^y{}^T S_L\right)^T - \mathbf{e}^T \left(V\Lambda^{1/2} \sum_{i=1}^{\beta} \kappa_i^{-1} \mathbf{b}_i^y \mathbf{d}_i^y{}^T\right)^T\right)\right\} \quad (A2) \\ &= \left(\mathbf{I} - V\Lambda^{1/2} \sum_{i=1}^{\beta} \kappa_i^{-1} \mathbf{b}_i^y \mathbf{d}_i^y{}^T S_L\right) E\{\mathbf{r} \mathbf{r}^T\} \\ &\quad \times \left(\mathbf{I} - V\Lambda^{1/2} \sum_{i=1}^{\beta} \kappa_i^{-1} \mathbf{b}_i^y \mathbf{d}_i^y{}^T S_L\right)^T \\ &\quad + \left(V\Lambda^{1/2} \sum_{i=1}^{\beta} \kappa_i^{-1} \mathbf{b}_i^y \mathbf{d}_i^y{}^T\right) E\{\mathbf{e} \mathbf{e}^T\} \left(V\Lambda^{1/2} \sum_{i=1}^{\beta} \kappa_i^{-1} \mathbf{b}_i^y \mathbf{d}_i^y{}^T\right)^T. \quad (A3) \end{aligned}$$

Note that an operator $E\{\bullet\}$ operates only on surface reflectances and noise. The relation of $E\{\mathbf{e} \mathbf{r}^T\} = E\{\mathbf{r} \mathbf{e}^T\} = 0$ is used in this equation, since the noise and the surface reflectances are uncorrelated. If the spectral reflectances of the learning samples are the same for test samples, then $E\{\mathbf{r} \mathbf{r}^T\} = V\Lambda V^T$. Let denote the first and second term on the right hand side of (A3) FT and ST, respectively. The use of the relation of Eq.(4) leads for FT,

$$\begin{aligned} FT &= V\Lambda V^T - V\Lambda^{1/2} \sum_{i=1}^{\beta} \kappa_i^{-1} \mathbf{b}_i^y \mathbf{d}_i^y{}^T S_L^y \Lambda^{1/2} V^T - V\Lambda^{1/2} \sum_{i=1}^{\beta} S_L^y{}^T \kappa_i^{-1} \mathbf{d}_i^y \mathbf{b}_i^y{}^T \Lambda^{1/2} V^T \\ &\quad + \sum_{i=1}^{\beta} \sum_{j=1}^{\beta} \kappa_i^{-1} \kappa_j^{-1} V\Lambda^{1/2} \mathbf{b}_i^y \mathbf{d}_i^y{}^T S_L^y S_L^j{}^T \mathbf{d}_j^y \mathbf{b}_j^y{}^T \Lambda^{1/2} V^T \quad (A4) \end{aligned}$$

Using relations of the singular value decomposition of S_L^y again,

i.e., $S_L^y = \sum_{i=1}^{\beta} \kappa_i^y \mathbf{d}_i^y \mathbf{b}_i^y{}^T$, and orthogonal normality of singular vectors leads to

$$FT = V\Lambda V^T - \sum_{i=1}^{\beta} V\Lambda^{1/2} \mathbf{b}_i^y \mathbf{b}_i^y{}^T \Lambda^{1/2} V^T \quad (A5)$$

Using the orthogonal normality of singular vectors of S_L^y , the second term ST can be written as

$$ST = \sum_{i=1}^{\beta} \sum_{j=1}^{\beta} \kappa_i^{-1} \kappa_j^{-1} V\Lambda^{1/2} \mathbf{b}_i^y \mathbf{d}_i^y{}^T R_{cc} \mathbf{d}_j^y \mathbf{b}_j^y{}^T \Lambda^{1/2} V^T \quad (A6)$$

Combining Eqs. (A5) and (A6) leads to Eq. (9)

$$\begin{aligned} A(0, R_{cc}) &= V\Lambda V^T - \sum_{i=1}^{\beta} V\Lambda^{1/2} \mathbf{b}_i^y \mathbf{b}_i^y{}^T \Lambda^{1/2} V^T \\ &\quad + \sum_{i=1}^{\beta} \sum_{j=1}^{\beta} \kappa_i^{-1} \kappa_j^{-1} V\Lambda^{1/2} \mathbf{b}_i^y \mathbf{d}_i^y{}^T R_{cc} \mathbf{d}_j^y \mathbf{b}_j^y{}^T \Lambda^{1/2} V^T \quad (A7) \end{aligned}$$

The proof is completed.

References

- [1] G.Sharma and H.J.Trussell, "Figure of Merit for Color Scanners", *IEEE Trans. Image Processing*, vol.6, 990(1997).
- [2] H. Stark, "Image Recovery: Theory and Application", Academic Press, (1987).
- [3] A. Rosenfeld and A. C. Kak, "Digital Picture Processing", 2en ed., vol.1, New York: Academic Press, , pp.281-293,(1982).
- [4] W.K.Pratt, "Digital Image Processing", New York: John Wiley & Sons, pp.365-396,(1991).
- [5] M.J. Vrhel and H.J. Trussell, "Filter Considerations in Color Correction", *IEEE Trans. Image Processing*, vol.3, 147 (1994)
- [6] N. Shimano, "Evaluation of a multispectral image acquisition system aimed at reconstruction of spectral reflectances", *Optical Engin.*, vol.44, 107115-1(2005)
- [7] N. Shimano, "Application of a Colorimetric Evaluation Model to Multispectral Color Image Acquisition Systems", *Journal of Imaging Sci. and Technl.*, vol.49, 588(2005).
- [8] N. Shimano, "Recovery of Spectral Reflectances of Objects Being Imaged Without Prior Knowledge", *IEEE Trans. Image Processing*, vol.15, 1848(2006).
- [9] N. Shimano, K. Terai and M. Hironaga, "Recovery of spectral reflectances of objects being imaged by multispectral cameras", *J. Opt. Soc. Amer. A*, vol.24, 3211 (2007).
- [10] J.S.Taylor and N. Cristianini, "Kernel Methods for Pattern Analysis", Cambridge Univ. Press pp.12-17 (2004).
- [11] H.L.Shen and H.H.Xin, "Spectral characterization of a color scanner based on optimized adaptive estimation", *J. Opt. Soc. Amer. A*, vol.23, 1566(2006).
- [12] J.L.Nieves, E.M.Valero, S.M.C.Nascimento, J. H. Andrés, and J. Romero, "Multispectral synthesis of daylight using a commercial digital CCD camera", *Appl. Optics*, vol.44, 5696(2005).
- [13] D.L.Snyder, C.W.Helstrom and A.D.Lanterman, M. Faisal and R.L. White, "Compensation for readout noise in CCD images", *J. Opt. Soc. Amr. A*, vol.12, 272(1995).
- [14] P. D. Burns and R. S. Berns, "Image Noise and Colorimetric Precision in Multispectral Image Capture", *Proc. of 6th Color Imag. Conf.*,83(1998).
- [15] H. Haneishi, T. Hasegawa, N. A. Hosoi, Y. Yokoyama, N.Tsumura and Y. Miyake, "System design for accurately estimating the spectral reflectance of art paintings", *Appl. Optics*, vol.39, 6621(2000).

- [16] P.L.Vora, J.E.Farrell, J.D.Tietz and D.H.Brainard, "Image Capture: Simulation of Sensor Responses from Hyperspectral Images", *IEEE Trans. Image Processing*, vol.10,307(2001).
- [17] J.W.Choi, M.G.Kang and K.T.Park,"An Algorithm to Extract Camera-Shaking Degree and Noise Variance in the Peak-Trace Domain", *IEEE. Trans. Consumer Electronics*, vol.44, 1159(1998).
- [18] T.S.Choi and S.O.Park,"A New Method for Focused Image Recovery from Image Defocus", *Proc. SPIE* , vol.3164,16(1997).

Author Biography

Noriyuki Shimano received his BE degree in electronics from Doshisha University, Kyoto, Japan in 1970, and ME and PhD degrees in electronics from Osaka Prefecture University, Osaka, Japan, in 1973 and in 1980, respectively. He is currently a professor in the department of informatics, Kinki University, Osaka. His research interests include physics-based vision, image and signal processing for the digital archive of art objects.